SANDIA REPORT

SAND2012-5845
Unlimited Release
Printed July 2012

Propagation of Model Form Uncertainty for Thermal Hydraulics using RANS Turbulence Models in Drekar

Michael S. Eldred and Timothy M. Wildey

Prepared by
Sandia National Laboratories
Albuquerque, New Mexico 87185 and Livermore, California 94550

Sandia National Laboratories is a multi-program laboratory managed and operated by Sandia Corporation, a wholly owned subsidiary of Lockheed Martin Corporation, for the U.S. Department of Energy's National Nuclear Security Administration under contract DE-AC04-94AL85000.

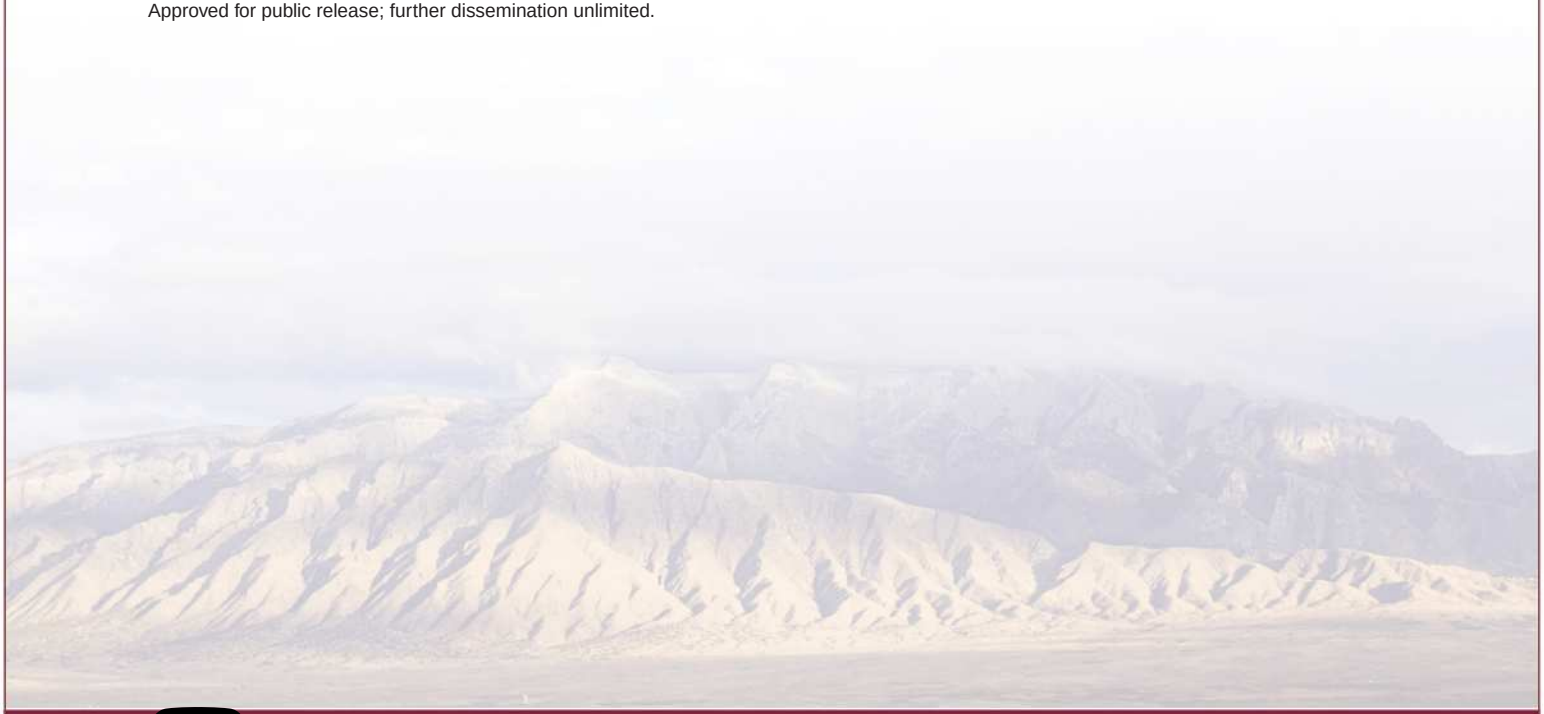

Issued by Sandia National Laboratories, operated for the United States Department of Energy by Sandia Corporation.

Available to DOE and DOE contractors from
U.S. Department of Energy
Office of Scientific and Technical Information
P.O. Box 62
Oak Ridge, TN 37831

Telephone: (865) 576-8401
Facsimile: (865) 576-5728
E-Mail: reports@adonis.osti.gov
Online ordering: http://www.osti.gov/bridge

Available to the public from
U.S. Department of Commerce
National Technical Information Service
5285 Port Royal Rd
Springfield, VA 22161

Telephone: (800) 553-6847
Facsimile: (703) 605-6900
E-Mail: orders@ntis.fedworld.gov
Online ordering: http://www.ntis.gov/help/ordermethods.asp?loc=7-4-0#online

SAND2012-5845
Unlimited Release
Printed July 2012

Propagation of Model Form Uncertainty for Thermal Hydraulics using RANS Turbulence Models in Drekar

Michael S. Eldred and Timothy M. Wildey
Optimization and Uncertainty Quantification Department
Sandia National Laboratories
P.O. Box 5800
Albuquerque, NM 87185-1318
mseldre@sandia.gov, tmwilde@sandia.gov

Abstract

This document summarizes the results from a level 3 milestone study within the CASL VUQ effort. It demonstrates the propagation of model form uncertainty that arises from the presence of multiple turbulence models within the context of thermal hydraulics analyses. The lack of knowledge associated with an inability to *a priori* identify an appropriate turbulence model is modeled as discrete epistemic uncertainty. This approach provides an alternative to model selection processes, for use when data is unavailable or inadequate for reducing the model form uncertainty. In this case, the alternative is to propagate the model form uncertainty and report UQ results that include this epistemic uncertainty source alongside other parametric sources. The study calculates epistemic intervals on aleatory statistics for several quantities of interest, where the epistemic intervals are computed using mixed continuous-discrete optimization methods and the aleatory statistics are computed using polynomial chaos expansions. We first investigate two simple algebraic test problems with multiple model forms and then deploy the methods to the Drekar thermal hydraulics application. The Drekar study employs a set of Reynolds-averaged Navier-Stokes (RANS) turbulence models, including Spalart-Allmaras and k-ε. Results highlight the utility of employing efficient mixed continuous-discrete optimizers based on surrogate emulation.

Acknowledgment

The authors thank the Drekar team, especially Tom Smith, John Shadid, and Eric Cyr, for delivering the thermal hydraulics examples used in this study. We also thank Patty Hough for assisting with the mixed-integer evolutionary algorithms in COLINY and Keith Dalbey for assisting with Gaussian process models in Surfpack.

Contents

Figures

Tables

1 Background

Uncertainty quantification (UQ) is the process of determining the effect of input uncertainties on response metrics of interest. These input uncertainties may be characterized as either aleatory uncertainties, which are irreducible variabilities inherent in nature, or epistemic uncertainties, which are reducible uncertainties resulting from a lack of knowledge. Since sufficient data is available for characterizing aleatory uncertainties, probabilistic methods are commonly used for computing response distribution statistics based on input probability distribution specifications. Conversely, for epistemic uncertainties, data is generally too sparse to support objective probabilistic input descriptions, leading either to subjective probabilistic descriptions (e.g., assumed priors in Bayesian analysis) or nonprobabilistic methods based on interval specifications (e.g., pure intervals or Dempster-Shafer basic probability assignments).

In this milestone, we are interested in the propagation of a mixture of aleatory and epistemic uncertainties, where the epistemic uncertainties include discrete parameterizations of model form. A common approach to quantifying the effects of mixed aleatory and epistemic uncertainties is to separate the aleatory and epistemic variables and perform nested iteration. From an algorithmic standpoint, this separation allows the use of strong probabilistic inferences where possible, while employing alternative inferences only where necessary. From a conceptual standpoint, the epistemic portion should capture uncertainty that is fully reducible (to constants) given perfect information, and the aleatory portion should capture all of the irreducible variability. To perform this separation rigorously, it may be necessary to separate aleatory and epistemic portions within a single random source, e.g. by modeling an aleatory random variable that is parameterized by an epistemic mean. Given this rigorous separation, the interpretation of the results of the nested iteration becomes straightforward: any particular epistemic realization represents a possible state of the full variability of the uncertain process. If the separation is not performed in this manner and irreducible uncertainty is hidden within the epistemic parameterization, then the results are more opaque: an epistemic realization is instead a partial expectation involving a subset of the actual random variability. Statistics derived from these partial expectations can be misleading and are easily misinterpreted; moreover, this mistake apears to be widespread due to the additional sophistication required to perform a rigorous separation.

It can be argued that model form uncertainty readily conforms to a rigorous epistemic separation in that we do not typically view it as having underlying stochastic variability; rather, in a perfect state of information and modeling, we would reduce to a single correct model form. Since, in reality, we do not have access to this perfect model form, we instead try to capture a representative range (i.e., an epistemic interval) of the possible model outcomes using the set of imperfect models that we have available. This is of course not guaranteed to bound the perfect model case, but rather provides a quantitative assessment of the uncertainty reflected within the current model form ensemble when we lack the data necessary to perform an informed model down-selection.

Traditionally, the analysis of mixed aleatory and epistemic uncertainty has involved a nested sampling approach, in which each sample drawn from the epistemic variables on the outer loop results in a sampling over the aleatory variables on the inner loop. In this fashion, we generate families or ensembles of response distributions, where each distribution represents the irreducible

aleatory uncertainty. Plotting an entire ensemble of cumulative distribution functions (CDFs) in a "horsetail" plot allows one to visualize the upper and lower bounds on the family of distributions (see Figure 1). However, nested iteration can be computationally expensive when it is implemented

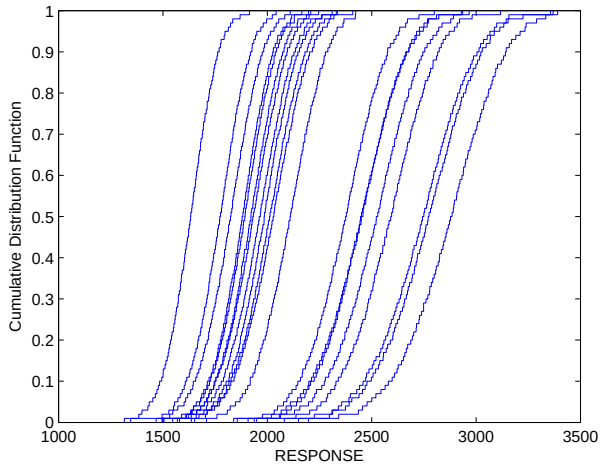

Figure 1. Example CDF ensemble. Commonly referred to as a "horsetail" plot.

using two random sampling loops. Consequently, when employing simulation-based models, the nested sampling must often be under-resolved, particularly at the epistemic outer loop, resulting in an under-prediction of credible output ranges.

In [3, 4], a central goal was to preserve the advantages of uncertainty separation while addressing issues with accuracy and efficiency by closely tailoring the algorithmic approaches to the propagation needs at each level. In particular, fast-converging stochastic expansion approaches (nonintrusive polynomial chaos and stochastic collocation) are employed for aleatory propagation, and optimization-based interval estimation is performed for the epistemic propagation. A significant amount of background information is provided in these references and is not repeated here; please refer to [3, 4] for additional information on polynomial chaos and stochastic collocation expansion methods for aleatory propagation and on interval-valued probability (IVP), Dempster-Shafer, and second-order probability (SOP) approaches for mixed UQ. In this report, we focus on the IVP formulation and build on the previous work to extend the optimization-based interval estimation approaches to include discrete epistemic parameterizations of model form.

2 Interval Estimation with Discrete Variables

In the IVP formulation, we seek the minima and maxima of aleatory statistical quantities of interest (QoI) over the epistemic parameters, where we extend the formulation in [3, 4] to include a mixture of continuous and discrete parameters:

$$\begin{aligned} \text{minimize} \quad & Q_i(\mathbf{c}, \mathbf{d}_r, \mathbf{d}_s) \\ \text{subject to} \quad & \mathbf{c}_L \leq \mathbf{c} \leq \mathbf{c}_U \\ & \mathbf{d}_L \leq \mathbf{d}_r \leq \mathbf{d}_U \\ & \mathbf{d}_s \in \mathbb{D} \end{aligned} \tag{1}$$

$$\begin{aligned} \text{maximize} \quad & Q_i(\mathbf{c}, \mathbf{d}_r, \mathbf{d}_s) \\ \text{subject to} \quad & \mathbf{c}_L \leq \mathbf{c} \leq \mathbf{c}_U \\ & \mathbf{d}_L \leq \mathbf{d}_r \leq \mathbf{d}_U \\ & \mathbf{d}_s \in \mathbb{D} \end{aligned} \tag{2}$$

where $\mathbf{Q}$ denotes the vector of QoI, $\mathbf{c}$ denotes the continuous epistemic parameters which are limited by real-valued bounds $[\mathbf{c}_L, \mathbf{c}_U]$, $\mathbf{d}_r$ denote discrete range parameters that are defined by a sequence of integers and are therefore limited by integer bounds $[\mathbf{d}_L, \mathbf{d}_U]$ on the sequence, and $\mathbf{d}_s$ denote discrete set parameters that are defined by finite sets of admissible real or integer values, one distinct admissible set per discrete parameter.

Since the QoI are nonlinear functions of the epistemic parameters in general, we require mixed-integer nonlinear programming (MINLP) solvers to compute solutions to these types of optimization problems. MINLP solvers are generally distinguished based on their support for categorial versus noncategorical discrete parameters. In the noncategorical case, the restriction to discrete values can be relaxed allowing the discrete parameters to take on continuous values during the solution process. An example of this type of approach is the branch and bound algorithm, which solves a series of continuous relaxation subproblems to compute bounds, prune branches, and ultimately arrive at a final solution which satisfies the restrictions to discrete values. When applicable, this type of approach is preferred due to computational efficiency, but it requires the ability to evaluate the model at non-discrete intermediate values. Thus, the more challenging case algorithmically is the case of categorical discrete variables, for which relaxed values cannot be simulated (e.g., 1.5 satellites in a constellation). The enumeration of model form choices generally falls into the categorical discrete variable case, such that relaxation-based algorithms are not directly applicable. MINLP for categorical variables must rely on combinatorial techniques and tends to be much more computationally expensive.

To enable MINLP with categorical variables to be applied for computationally expensive thermal hydraulics models, we leverage our capability for surrogate modeling, in particular Gaussian process (GP) modeling. In [3, 4], we utilize the prediction variance estimates of GPs to formulate approaches based on expected improvement. Continuous optimization based on maximizing

expected improvement functions from GPs is commonly known as efficient global optimization (EGO) [6], which can be a highly effective technique for balancing the competing desires to *explore* regions where little is known and *exploit* regions where promising solutions have already been found. Longer term, it is our intent to extend the EGO approach to support discrete parameters through a generalization to the expected improvement formulation.

For initial demonstration of IVP with categorical discrete parameters, we have initially focused on three algorithmic approaches for the interval estimation at the epistemic outer loop. First, as a benchmark and sanity check, we have the simple approach of employing Latin hypercube sampling [9] over the parameter set $\mathbf{c}, \mathbf{d}_r, \mathbf{d}_s$ and then reporting the observed minimum and maximum sample as the interval bounds. In this case, there is no adaptation or refinement, only a single randomly generated sample set.

Second, we can start from an initial random sample, and then evolve this population of candidate optima using a mixed-integer evolutionary algorithm. Here we apply the EAminlp solver from COLINY [5] directly to the simulation model, with no surrogate emulation.

Third, we combine the LHS and EAminlp solvers with adaptive surrogate emulation. We have implemented an adaptive surrogate-based global optimization (SBGO) approach that takes an initial LHS sample, forms a set of GP models for the epistemic QoI, and then iteratively adapts each GP while computing approximate minima and maxima using EAminlp. In particular, the SBGO approach involves the following steps:

1. Perform LHS over the range of the parameter set $\mathbf{c}, \mathbf{d}_r, \mathbf{d}_s$ and form initial GP models for the quantities of interest $\mathbf{Q}$ at the epistemic outer loop. Each epistemic realization involves an aleatory UQ propagation.

2. Apply a categorical MINLP solver (in this case, EAminlp) to minimize the GP prediction to compute an approximate minimum. This solution is tested for soft convergence in terms of change in solution $\mathbf{c}^*, \mathbf{d}_r^*, \mathbf{d}_s^*$ and change in approximate QoI minimum. If converged, skip to step 4; else, continue to step 3.

3. the approximate minimum is validated with an aleatory analysis and the GP is updated with these truth model results. Return to step 2.

4. The MINLP solver is now applied to maximize the prediction of the adapted GP. Note that the previously-adapted GP can be fully reused, only the sense of the optimization is changed. This MINLP solution is tested for soft convergence; if converged, advance to the next QoI and return to step 2 (or stop if no more QoI); else, continue to step 5.

5. the approximate maximum is validated with an aleatory analysis and the GP is updated with these truth model results. Return to step 4.

Relative to the EGO approach for successive adaptation of GP models, SBGO strictly exploits regions with good solutions, and does not support global exploration beyond the initial GP construction in step 1.

3 Computational Experiments

Two simple algebraic tests are included to demonstrate algorithm behavior and relative performance in greater detail. For these problems, distinct model forms are drawn from previously published multifidelity examples; although all fidelities are treated as model form peers in this context. We conclude with the targeted thermal hydraulics application using Drekar, demonstrating the approach for CASL-relevant physics.

3.1 Rosenbrock example

We start with a simple example of two model forms for the Rosenbrock polynomial, originally published in [2]:

$$\text{Form 1}: \quad f_1 = 100(x_2 - x_1^2)^2 + (1 - x_1)^2 \tag{3}$$

$$\text{Form 2}: \quad f_2 = 100(x_2 - x_1^2 + .2)^2 + (0.8 - x_1)^2 \tag{4}$$

where form 1 is the traditional polynomial and the small offsets in form 2 are sufficient for it to differ from form 1 in function, gradient, and Hessian values. The two variables are independent standard normals, and aleatory metrics include the mean and standard deviation of f.

If only the model form were epistemic, then the interval optimization could be performed by simple enumeration of two aleatory analyses, one for each model form. In this case, the epistemic intervals for aleatory mean and standard deviation of f using an aleatory sparse grid level of two would be $[365.64, 402.00]$ and $[997.52, 1050.0]$, respectively. To make the example more interesting, we add continuous epistemic variables that define the means of the aleatory random variables x_1 and x_2. In particular, $x_1 \sim N(\mu_1, 1), x_2 \sim N(\mu_2, 1)$ with $\mu_1 \in [-1, 1], \mu_2 \in [-1, 1]$. These results are reported in the following three sections.

3.1.1 UQ Results: LHS

Table 1 shows Latin hypercube sampling results for the Rosenbrock example, again using an aleatory sparse grid level of two. It is evident that the intervals are converging (lower bounds from above and upper bounds from below), but only appear to be accurate to a few digits after extensive sampling (10^5 outer loop samples with greater than two million total evaluations).

3.1.2 UQ Results: EA

Table 2 shows results for mixed-integer evolutionary optimization with the population size set to 100 and the maximum number of population cycles for each QoI bound set to 5, 10, and 25 (corresponding to 2380, 4360, and 10300 total outer loop evaluations, respectively). Note that any

Table 1. UQ results using LHS for Rosenbrock example.

Outer Evals	Total Evals	μ_f	σ_f
10	210	[346.152, 1153.31]	[1005.22, 2552.71]
100	2100	[303.160, 1385.31]	[796.943, 2861.09]
1000	21000	[302.098, 1524.23]	[789.075, 3005.77]
10000	210000	[301.680, 1579.54]	[777.004, 3097.92]
100000	2100000	[301.656, 1602.87]	[776.399, 3122.45]

simulation duplicates are not re-evaluated, such that the total evaluations reported reflect unique simulation counts. It is evident that the intervals are converging more rapidly than for LHS, as

Table 2. UQ results using EA for Rosenbrock example.

Outer Evals	Total Evals	μ_f	σ_f
2380	44457	[302.003, 1605.00]	[778.958, 3124.36]
4360	69283	[301.998, 1605.00]	[776.052, 3124.36]
10300	99869	[301.638, 1605.00]	[776.109, 3124.36]

would be expected when using directed optimization techniques. The EA intervals after approximately 10^5 total evaluations are more converged than those after 2.1 million total LHS evaluations. However, even after a reduction of a factor of 20, the EA function evaluation counts are still unacceptably high for use in expensive CASL applications.

3.1.3 UQ Results: SBGO

Table 3 shows results for surrogate-based global optimization for three different initial sample sizes: 10, 20, and 100 random initial LHS points (corresponding to 27, 33, and 113 outer loop evaluations after refinement). As for the EA, simulation duplicates are not re-evaluated such that the total evaluations reflect unique simulations. The first result (27 outer loop evaluations) starts from

Table 3. UQ results using SBGO for Rosenbrock example.

Outer Evals	Total Evals	μ_{f_1}	σ_{f_1}
27	546	[302.001, 1601.00]	[776.062, 3121.79]
33	683	[301.640, 1605.00]	[776.044, 3121.79]
113	2352	[301.638, 1605.00]	[776.044, 3124.36]

the same data as the 10 outer loop sample case in Table 1, and it is evident that the optimization-driven refinement significantly improves the accuracy of the bounds with relatively few additional

evaluations. The third result (2352 total evaluations) has comparable accuracy to 10^5 total evaluations for the EA and is more converged than 2.1 million total LHS evaluations, using 2.4% and 0.11% of the total evaluation cost, respectively. These evaluation counts are much more practical for use with Drekar.

Taking an EA result after 50 population cycles as a reference solution, we plot the convergence rates for each of the three techniques in Figure 2. Relative errors are averaged over the four QoI and the three SBGO results are shown initiated from the LHS sample sets (10, 20, and 100 outer loop evaluations) used to construct their initial GPs. It is evident that the convergence rates for SBGO and EA are much faster than LHS, and the convergence of the SBGO refinement becomes more rapid as the initial GP approximation becomes more accurate.

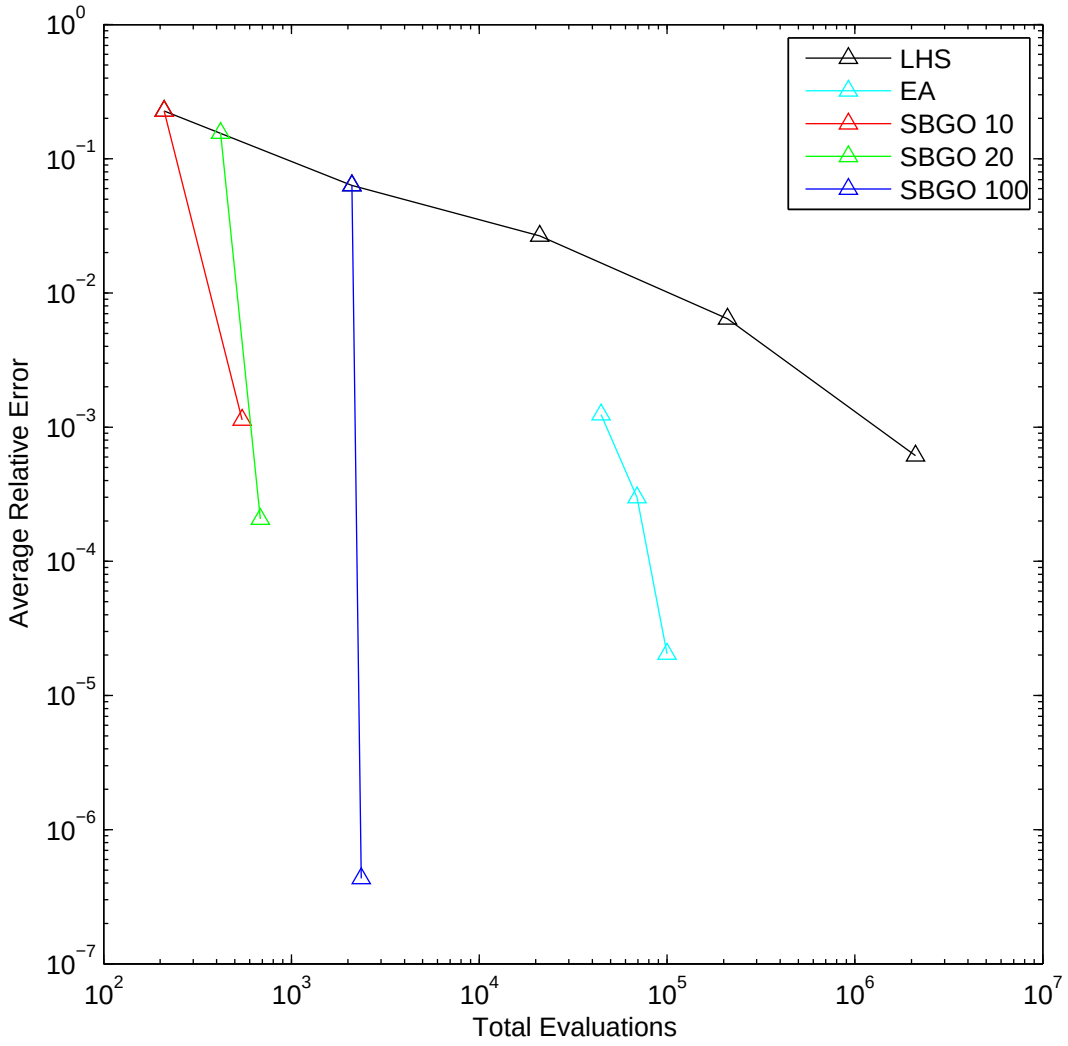

Figure 2. Convergence of MINLP approaches for Rosenbrock example.

3.2 Short column example

Relative to the previous example, this test problem increases the aleatory dimension from two to five, increases the number of model form alternatives from two to four, and replaces polynomials with rational functions within the model forms. It involves the plastic analysis and design of a short column [7] with rectangular cross section (width b and depth h), having uncertain material properties (yield stress Y), and subject to uncertain loads (bending moment M and axial force P). The model forms for the limit state are:

$$\text{Form 1}: \quad f_1 = 1 - \frac{4M}{bh^2Y} - \left(\frac{P}{bhY}\right)^2 \tag{5}$$

$$\text{Form 2}: \quad f_2 = 1 - \frac{4P}{bh^2Y} - \left(\frac{P}{bhY}\right)^2 \tag{6}$$

$$\text{Form 3}: \quad f_3 = 1 - \frac{4M}{bh^2Y} - \left(\frac{M}{bhY}\right)^2 \tag{7}$$

$$\text{Form 4}: \quad f_4 = 1 - \frac{4M}{bh^2Y} - \left(\frac{P}{bhY}\right)^2 - \frac{4(P-M)}{bhY} \tag{8}$$

where Form 1 is the traditional form and Forms 2–4 were published in [8]. The distributions of the random variables are uniform for b and h ($[5,15]$ and $[15,25]$, respectively), normal for P and M (nominally $N(500,100)$ and $N(2000,400)$, respectively), and lognormal for Y (nominally $(\mu,\sigma) = (5,.5)$). P and M are correlated with a correlation coefficient of 0.5 (uncorrelated otherwise).

We again augment the discrete epistemic model form variable with continuous epistemic variables that define the means of the aleatory random variables P, M, and Y. In particular, $P \sim N(\mu_P,100), M \sim N(\mu_M,400), Y \sim logN(\mu_Y,0.5)$ with $\mu_P \in [400,600], \mu_M \in [1750,2250], \mu_Y \in [4,6]$. The aleatory metrics are again the mean and standard deviation of f, where the aleatory moments are evaluated using a polynomial chaos expansion with a sparse grid level of two (requiring 77 evaluations for five variables using a Wiener-Askey basis (Hermite and Legendre basis polynomials) and nested quadrature rules (Genz-Keister and Gauss-Patterson)).

3.2.1 UQ Results: LHS

Table 4 shows Latin hypercube sampling results for the short column example. As for the previous example, the LHS results appear to be converging, although the rate is slow with only a few digits of accuracy after extensive sampling (10^5 outer loop samples and 7.7 million total evaluations).

3.2.2 UQ Results: EA

Table 5 shows results for mixed-integer evolutionary optimization with the population size set to 100 and the maximum number of population cycles for each QoI bound set to 5, 10, 25, and 50.

Table 4. UQ results using LHS for short column example.

Outer Evals	Total Evals	μ_f	σ_f
10	770	[-7.17261, 8.44924]	[0.221240, 7.40993]
100	7700	[-9.67710, 9.83783]	[0.227391, 9.40208]
1000	77000	[-10.9394, 9.86118]	[0.208164, 10.3996]
10000	770000	[-11.6426, 10.0846]	[0.203038, 11.0640]
100000	7700000	[-11.7292, 10.2398]	[0.203071, 11.1351]

Duplicates are again removed from the total evaluation counts. Compared to LHS, the EA results

Table 5. UQ results using EA for short column example.

Outer Evals	Total Evals	μ_f	σ_f
2380	181951	[-11.8079, 9.10378]	[0.214753, 11.2011]
4360	327943	[-11.8079, 9.97481]	[0.202296, 11.2011]
10300	703837	[-11.8079, 9.96541]	[0.202296, 11.2011]
20200	1113730	[-11.8079, 10.1737]	[0.202296, 11.2011]

with approximately 10^4 outer loop samples can be seen to be more converged than those for 10^5 outer loop LHS samples for three of the four results (μ_f upper bound is the exception), again showing benefit in optimization-based approaches. However, the total number of evaluations is still prohibitive for use with thermal-hydraulics codes such as Drekar.

3.2.3 UQ Results: SBGO

Table 6 shows results for surrogate-based global optimization with initial samples set at 10, 20, and 100 and the maximum number of refinement iterations for each QoI bound set to 10. It is evident

Table 6. UQ results using SBGO for short column example.

Outer Evals	Total Evals	μ_f	σ_f
35	2541	[-11.8079, 10.3277]	[0.202296, 11.2011]
50	3619	[-11.8079, 10.3277]	[0.202296, 11.2011]
122	9240	[-11.8079, 10.3277]	[0.202296, 11.2011]

that 10 initial samples are sufficient for global accuracy in this problem and that the additional exploration provided by the 20 and 100 initial sample sets provided no incremental benefit in this case. The results for SBGO are the most accurate for each of the four bounds (addressing the μ_f upper bound inaccuracy that occurred for the direct EA case) and come at a fraction of the expense: the SBGO result with 2541 total evaluations is obtained for 0.23% of the cost of the best

EA solution and for 0.033% of the most converged LHS result. Again, these evaluation reductions are critical for exploration of model form issues with expensive CFD models.

Taking an EA result after 100 population cycles as a reference solution, we plot the convergence rates for each of the three techniques in Figure 3. Relative errors are averaged over the four QoI and the SBGO result is shown initiated from the LHS sample set (10 outer loop evaluations) used to construct its initial GP. It is evident that, while the EA demonstrates some improvement over LHS, the SBGO approach demonstrates convergence that is superior to both.

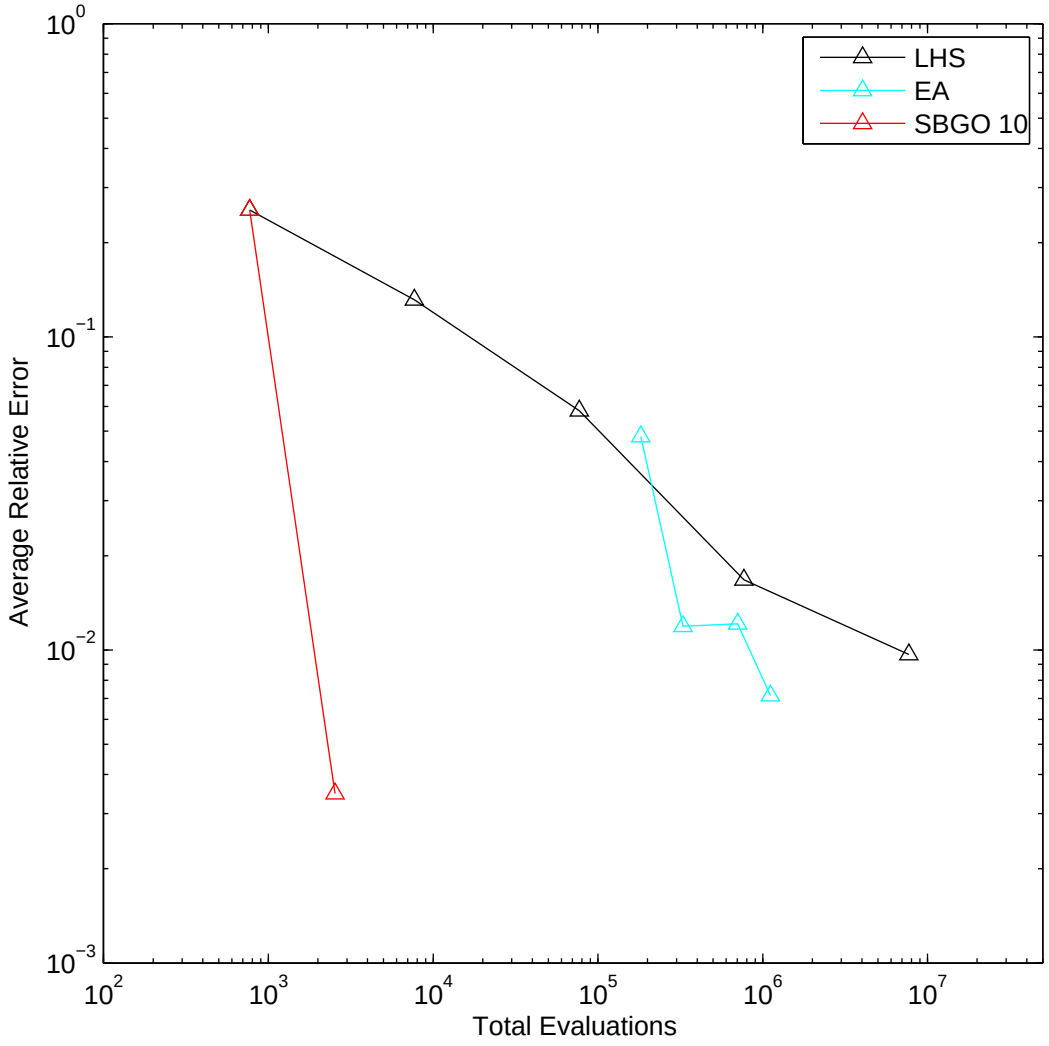

Figure 3. Convergence of MINLP approaches for short column example.

3.3 Thermal Hydraulics with Drekar

Fuel rods within light-water nuclear reactors are cooled from water flowing through the core. Turbulence within these fluid flows has a significant effect on cooling effectivness, yet the modeling of turbulence is not a mature science; significant uncertainty exists in turbulence model formulations and a relatively large family of candidates exist.

In this study, RANS turbulence models are explored within the framework of the Drekar simulation code. At this time, two models were viewed as being sufficiently mature and robust with respect to parameter variations for this study: the Spalart-Allmaras (SARANS) model and the k-ε (KERANS) model with Neumann boundary conditions for the turbulent kinetic energy (TKE).

In this study, we consider flow in a 3D channel as shown in Figure 4. The mesh is much finer along the top and bottom boundaries to efficiently resolve the near-wall region. We enforce a pressure drop in the x-direction via a source term in the Navier Stokes equations. No-slip boundary conditions ($\mathbf{u} = \mathbf{0}$) are enforced along the top and bottom boundaries, while the remaining boundaries are chosen to be stress-free. In Figure 5 we plot the x-velocity for a typical realization computed using a SARANS model, and in Figure 6 we plot the profile of the x-velocity along the outflow boundary.

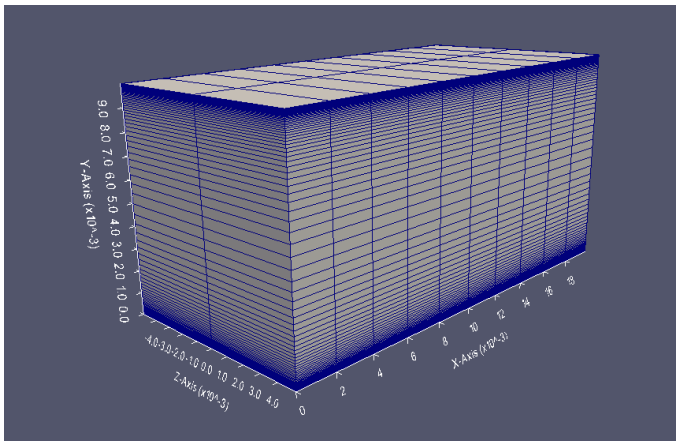

Figure 4. The steady-state x-velocity for typical realization computed using a RANS model in Drekar.

We consider the molecular viscosity (denoted by ν) and the source term for the x-momentum equation (denoted by f) to be aleatoric uniform random variables with epistemic upper bounds: $\nu \sim U(1E-5, \eta_\nu)$ and $f \sim U(10, \eta_f)$ with $\eta_\nu \in [5e-5, 5e-4]$ and $\eta_f \in [20, 40]$. Our simulation quantities of interest are the spatially averaged x-velocity and the spatially averaged pressure. The aleatory statistics of interest are the stochastic means of these simulation QoI, and we seek epistemic intervals on these aleatory statistics computed over model form, η_ν and η_f.

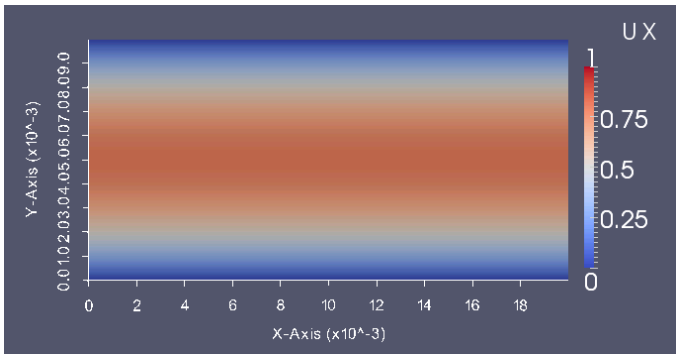

Figure 5. The steady-state x-velocity for typical realization computed using a RANS model in Drekar.

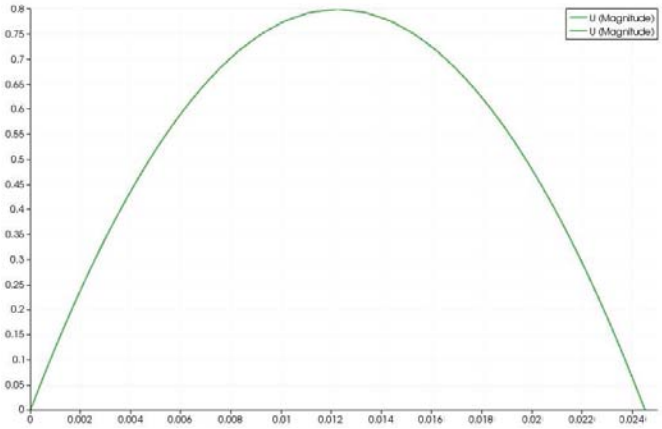

Figure 6. The profile of of the steady-state x-velocity along the outflow boundary for a typical realization computed using a RANS model in Drekar.

3.3.1 UQ Results

We start with 10 Latin hypercube samples on the epistemic outer loop, and employ 5^{th}-order tensor quadrature (4^{th}-order tensor polynomial chaos expansions) within each inner loop aleatory propagation. SBGO adapts this initial sample based on sequential application of the EA to a GP emulator. Table 7 summarizes the results for these two methods. Direct application of the EA without GP emulation was cost prohibitive and was not attempted. SBGO shows significant refinement in all four bounds. Although we do not have a reference solution in this case, it is safe to assume that the broadened intervals for μ_{ux} and $\mu_{pressure}$ from SBGO are more representative of the true epistemic range than those from the coarse initial sampling. Running 425 Drekar simulations for this simple

Table 7. UQ results for Drekar channel flow problem

Method	Outer Evals	Total Evals	μ_{ux}	$\mu_{pressure}$
LHS	10	250	[0.727604, 2.78150]	[32.6109, 282.237]
SBGO	17	425	[0.622869, 4.44624]	[21.7321, 297.957]

geometry could be completed in about 10.4 hours on a single workstation using 8 cores.

For the SBGO results, the KERANS model form provided the lower bound for μ_{ux} and the upper bound for $\mu_{pressure}$, while the SARANS model form provided the upper bound for μ_{ux} and the lower bound for $\mu_{pressure}$.

4 Observations

Deployment of discrete epistemic parameterizations for propagating model form uncertainty has led to the following primary observations:

- In each of the computational experiments, clear benefit was shown in utilizing optimization approaches relative to LHS sampling. In the Rosenbrock example, a cost reduction of a factor of 20 was observed for the EA in achieving comparable accuracy, which rose to a factor of 1000 for SBGO. In the short column example, the EA provided more converged results for three out of four bounds with an order of magnitude fewer total evaluations, while SBGO provided the most accurate results for all four bounds with a factor of 3000 reduction in total evaluation cost. And in the Drekar example, significant refinement in all four bounds was demonstrated for SBGO relative to LHS (intervals for μ_{ux} and $\mu_{pressure}$ broadened by 86% and 11%, respectively), using only seven additional outer loop evaluations.

- The application of standard emulation techniques, such as Gaussian process modeling, to mixed continuous-discrete domains can be challenging for problems where different discrete values result in radically different response behavior. In this work, we treated the discrete model form parameter as if it were a continuous parameter within the surrogate construction process, but with the restriction that only the allowable discrete values were visited. For the three problems studied, this approach was sufficient and the continuously-parameterized GP models were predictive of the model form variation. However, more explicit management of discrete emulation (with alternative correlation formulations) is expected to be necessary for supporting general application needs in this area. Current Sandia LDRD projects and associated external academic collaborations have been focusing on the discrete emulation challenge, such that a number of directions are possible for evolving discrete GP emulation capabilities within our interval estimation techniques.

- In parallel to the discrete GP emulation capability, extensions to the adaptive refinement machinery are also envisioned. Unlike the EGO-based approach for continuous epistemic parameters, the SBGO algorithm for mixed epistemic parameters is purely exploitative and lacks any adaptive refinement pressure for exploring regions that may contain good solutions. The SBGO approach must rely on the initial LHS sample for exploration of the space. For this reason, SBGO is not expected to be as reliable in identifying global optima as EGO is in [3, 4], since all regions of the parameter space may not be adequately explored. Extension of the EGO-based approach to support discrete epistemic parameters is of interest in future work.

- In this study, we have enumerated different model form options from a single modeling source. However, it is for more complex multi-component simulations (e.g., multiphysics simulation of reactor cores) for which manual enumeration becomes impractical and the automation and greater efficiency within these approaches can provide the greatest benefit. To fully realize this potential, additional improvements such as those described above will be needed to offset the combinatorial growth in complexity.

- This study has assumed that the aleatory parameterizations are common among the different model forms. For cases where different outer loop model form selections result in different inner loop parameterizations, the interval estimation procedure can still be performed, but the software infrastructure will require modification to additionally allow alternation of aleatory uncertainty specifications. Further explorations with Drekar could exercise this capability, given differences in the parameterization of different turbulence model forms.

In addition, the following algorithmic details are noted:

- The order of GP trend functions was an issue when the number of model alternatives was small. In particular, use of a quadratic trend was problematic when only two model alternatives were present. A restriction to a linear trend function was enforced.
- EA performance was not carefully optimized for direct application without emulation. For example, initial population sizes were large and could be better optimized for efficiency.

To further build on this initial discrete interval estimation capability, the following additional directions could be pursued:

- The gradient-enhanced kriging (GEK) capability could be employed at the outer epistemic loop to incorporate sensitivies of the aleatory statistics with respect to the continuous epistemic parameters, as enabled by the underlying stochastic expansions [1, 4]. This extension would enable greater scalability with respect to continuous epistemic dimension.
- Goal-oriented adaptive refinement can be employed on the aleatory inner loop to enable more efficient resolution of the aleatory QoI for particular epistemic realizations. Each of the computational experiments employed a fixed isotropic resolution for the aleatory random variables, but additional performance optimizations are possible and would be essential for higher dimensional aleatory propagations.
- Extension from IVP to Dempster-Shafer is straightforward, but has not been explored in this work. Similar to the increasing combinatorial complexity envisioned for multiphysics, the combinatorial growth in cell counts that can occur with finely-discretized Dempster-Shafer structures can potentially be offset by exploring opportunities listed previously for improving the efficiency and robustness of the core interval estimation components.

References

[1] M. S. Eldred. Design under uncertainty employing stochastic expansion methods. *International Journal for Uncertainty Quantification*, 1(2):119–146, 2011.

[2] M. S. Eldred, A. A. Giunta, and S. S. Collis. Second-order corrections for surrogate-based optimization with model hierarchies. In *Proceedings of the 10th AIAA/ISSMO Multidisciplinary Analysis and Optimization Conference*, Albany, NY,, Aug. 30–Sept. 1, 2004. AIAA Paper 2004-4457.

[3] M. S Eldred and L. P. Swiler. Efficient algorithms for mixed aleatory-epistemic uncertainty quantification with application to radiation-hardened electronics. part 1: Algorithms and benchmark results. Technical Report SAND2009-5805, Sandia National Laboratories, Albuquerque, NM, 2009.

[4] M. S. Eldred, L. P. Swiler, and G. Tang. Mixed aleatory-epistemic uncertainty quantification with stochastic expansions and optimization-based interval estimation. *Reliability Engineering and System Safety*, 96(9):1092–1113, 2011.

[5] W. E. Hart. The coliny project. Web site, 2007. `http://software.sandia.gov/Acro/Coliny/`.

[6] D. Jones, M. Schonlau, and W. Welch. Efficient global optimization of expensive black-box functions. *J. Global Optimization*, 13:455–492, 1998.

[7] N. Kuschel and R. Rackwitz. Two basic problems in reliability-based structural optimization. *Math. Method Oper. Res.*, 46:309–333, 1997.

[8] L. W. T. Ng and M. S. Eldred. Multifidelity uncertainty quantification using nonintrusive polynomial chaos and stochastic collocation. In *Proceedings of the 14th AIAA Non-Deterministic Approaches Conference*, number AIAA-2012-1852, Honolulu, HI, April 23-26, 2012.

[9] L. P. Swiler and G. D. Wyss. A user's guide to Sandia's latin hypercube sampling software: LHS UNIX library and standalone version. Technical Report SAND04-2439, Sandia National Laboratories, Albuquerque, NM, July 2004.

DISTRIBUTION:

1	MS 1318	Brian M. Adams, 1441
1	MS 1318	Keith Dalbey, 1441
3	MS 1318	Michael S. Eldred, 1441
1	MS 1318	James R. Stewart, 1441
3	MS 1318	Timothy M. Wildey, 1441
1	MS 1320	Eric C. Cyr, 1426
1	MS 1320	Thomas M. Smith, 1442
1	MS 1321	John N. Shadid, 1444
1	MS 9159	Patricia D. Hough, 8954
1	MS 0899	Technical Library, 9536 (electronic copy)

Sandia National Laboratories